

A spherical gravitational wave detector readout by nearly quantum limited SQUIDs

M Podt¹, L Gottardi², A de Waard², G Frossati² and J Flokstra¹

¹ Faculty of Science and Technology, MESA + Research Institute, University of Twente, PO Box 217, 7500 AE Enschede, The Netherlands

² Kamerlingh Onnes Laboratory of the Leiden University, PO Box 9504, 2300 RA Leiden, The Netherlands

E-mail: j.flokstra@utwente.nl

Received 17 July 2003, in final form 24 September 2003

Published 13 November 2003

Online at stacks.iop.org/SUST/16/1531

Abstract

We are developing nearly quantum limited two-stage SQUID systems for the readout of the MiniGRAIL, the first spherical gravitational wave detector with a diameter of 65 cm and a mass of 1150 kg. The two-stage SQUID systems are based on a conventional dc SQUID as the sensor and a double relaxation oscillation SQUID (DROS) as the second stage. The SQUID systems will be coupled to the detector via a multi-mode inductive transducer. The large flux-to-voltage transfer of the two-stage SQUID system allows a direct voltage readout scheme, i.e. without (ac flux) modulation. At $T = 4.2$ K, the energy resolution in flux-locked loop was measured to be $\varepsilon = 27 h$, and at a temperature around 20 mK, the energy resolution is expected to reach the quantum limit.

1. Introduction

The MiniGRAIL is the first of three similar spherical gravitational wave detectors that will be operated in coincidence [1, 2]. The two other spherical detectors will be built in São Paulo [3] and in Rome. The MiniGRAIL is based on a CuAl6% sphere with a diameter of 65 cm and a mass of 1150 kg. The resonant frequency of the detector is 3 kHz, and the operation temperature will be around 20 mK. When the sphere is excited by a gravitational wave, it will show quadrupole modes of vibration. In order to measure the extremely small displacements (of the order of 10^{-20} m) related to these quadrupole deformations, two coupled mechanical resonators are used for amplification [4]. On top of the last resonator, a superconducting film is deposited. The displacement of the superconducting film modulates the persistent current in a superconducting circuit. The current variations are detected by a two-stage SQUID system based on a double relaxation oscillation SQUID (DROS) [5–7], as is schematically shown in figure 1.

Figure 2 shows the scheme of a two-stage SQUID system based on a DROS. The sensor SQUID is voltage biased, and the current I_1 is fed through the input coil of the DROS thereby

introducing a flux gain $G_\Phi = \partial\Phi_{2nd}/\partial\Phi_{sig}$. Here, Φ_{2nd} is the flux coupled to the second stage. The flux gain should be sufficiently large, such that the amplified flux noise of the sensor SQUID is larger than the noise contributions of the DROS and the room temperature readout electronics. Hence, in a well-designed two-stage SQUID system, the overall system noise is determined by the sensor SQUID.

As a result of the flux gain, one flux quantum in the sensor SQUID creates multiple modulation periods in the flux-to-voltage characteristic of the DROS, see figure 3. The large flux-to-voltage transfer of the two-stage SQUID system, typically $3 \text{ mV}/\Phi_0$ or larger, enables a direct voltage readout scheme without the overall system sensitivity being limited by the room temperature preamplifier [5]. Since no flux modulation is required for a two-stage SQUID system based on a DROS, the complexity of the flux locked loop (FLL) system can be considerably reduced compared to ac modulated SQUID systems.

In this paper, we discuss the readout of the MiniGRAIL and we present the current status of the development of nearly quantum-limited two-stage SQUID systems for the readout of the detector.

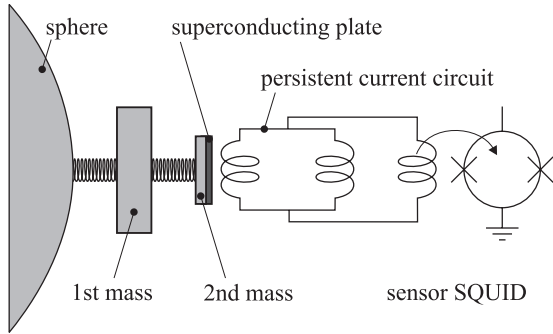


Figure 1. Schematic overview of the SQUID readout system for MiniGRAIL.

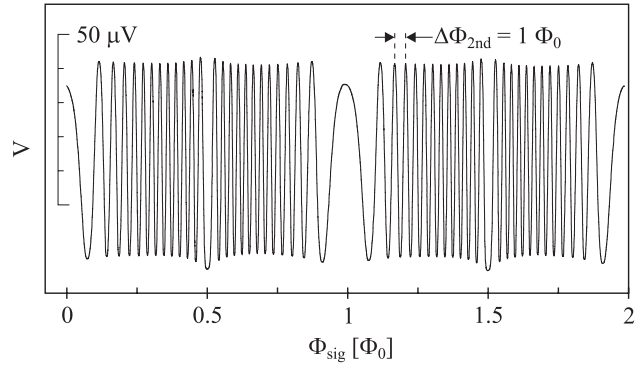


Figure 3. Typical experimental flux-to-voltage characteristic of a non-integrated two-stage SQUID system based on a dc SQUID as the sensor SQUID and a DROS as the second stage.

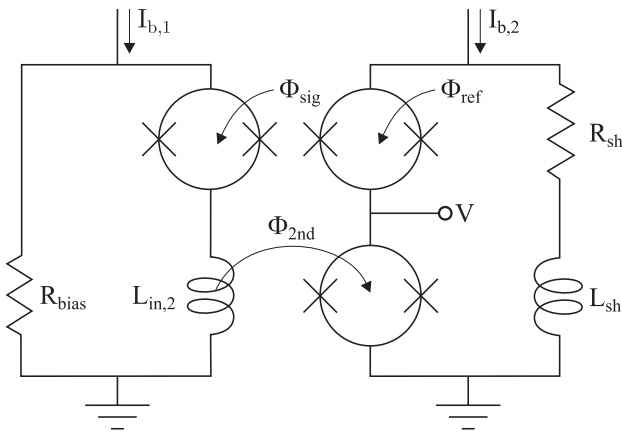


Figure 2. Scheme of a two-stage SQUID system based on a double relaxation oscillation SQUID (DROS) as the second stage.

2. MiniGRAIL

The main advantage of a spherical gravitational wave detector compared to the traditional resonant bar detectors is the omnidirectionality, which results in a large cross section [2]. A gravitational wave that interacts with the MiniGRAIL excites a combination of five spheroidal quadrupole modes of vibration. Operating at a temperature below 20 mK, the quantum limited strain sensitivity of MiniGRAIL is expected to be $\Delta L/L \approx 4 \times 10^{-21}$ for bursts, with a bandwidth of ~ 230 Hz.

At least six multi-mode mechanical resonators with a high quality factor will be used to detect the amplitude, the direction and the polarization of the gravitational waves. A two-mode resonator is under development [4]. The first resonator is made of CuAl6% and has an effective mass of about 450 g. The second mass consists of an Al5056 disc and has an effective mass of about 2 g. On top of this disc, a 600 nm Nb thin film is deposited using dc magnetron sputtering.

In front of the second resonator, a superconducting thin film Nb coil will be placed. A prototype Nb flat coil with an inductance of $L \approx 550$ nH and a thickness of 400 nm has been dc magnetron sputtered on a 2 inch Si wafer, see figure 4. The coil consists of a counter-wound spiral, i.e. a bifilar design, of 40 turns with a width and a pitch of 200 μm . In the final assembly, the coil will be placed in front of the second resonator at a distance of 20 μm . The effective inductance L_{eff} of the coil in this configuration has been calculated and measured to be of the order of 250 nH.



Figure 4. Photograph of the prototype Nb flat coil.

On the same wafer a superconducting heat switch is deposited. In order to test how much current could be stored in the coil in a persistent mode, a dc set current was put through the superconducting heat switch. After applying a short heat pulse to the switch, the current flows through the Nb coil, generating a voltage pulse. The current I_t that is trapped in the coil is determined by the integrated voltage V_c across the coil:

$$I_t = \frac{1}{L} \int V_c dt, \quad (1)$$

where L is the inductance of the coil. Figure 5 shows the integrated voltage across the coil as a function of the set current during charging and discharging of the coil. The maximum persistent current that could be stored in this coil was 4 A, and the critical current of the Nb film coil was 6.2 A. The lower value of the stored current is probably due to the fact that for higher currents the dissipation in the short Nb line, driven normal by the heat pulse, also warms up part of the coil itself. From the linear fit of the plot in figure 5, the value of the coil inductance was calculated using equation (1). The calculated value was $L = 550 \pm 20$ nH, which is in fair agreement with the value of 580 nH calculated by finite element analysis.

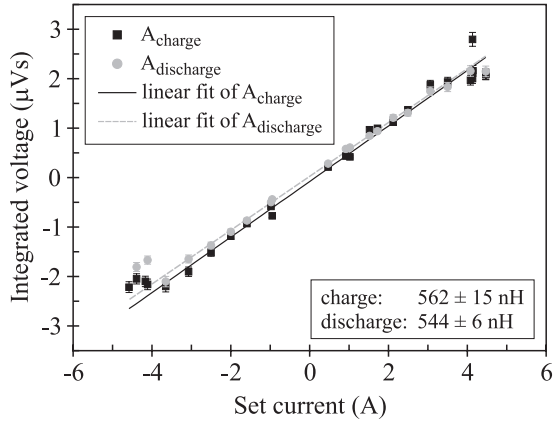


Figure 5. Integral of the voltage across the Nb flat coil as a function of the dc set current that was put through a superconducting switch. The integrated voltage determines the current trapped in the Nb coil.

Since the Nb film, which is deposited on top of the second resonator, screens the magnetic field generated by the coil, the effective self-inductance of the Nb coil is modulated by the movement of the second resonator. As a result of this movement and because of flux quantization in the persistent current circuit, a time-dependent current is superimposed on the persistent current in the coil. The time-dependent component is coupled to a two-stage SQUID system based on a DROS via a superconducting flux transformer.

In order to study the effect of a Nb film layer on the mechanical properties of the Al5056 resonator, we measured the quality factor of the resonator before and after the deposition of the film in a 4.2 K cryostat. The cryostat is equipped with a set of three spring-mass damping systems and two cantilever supports in order to isolate the resonator from mechanical vibration around the working frequency of 3.2 kHz. The anti-vibration system provides an attenuation of more than 150 dB in vacuum.

The aluminium resonator is press-fit, using thermal contraction techniques, inside a conic hole of a rigid CuAl support. To improve the clamping, three Al5056 screws are also used to fix the resonator vertically. The Al5056 resonator was electro discharge machined (EDM). It has a resonant frequency of 3256.4 Hz at 4.2 K and an effective mass of 1.5 g. Before the Nb film deposition and before any mechanical quality factor measurements, the top surface of the resonator was polished. We measured, using piezoelectric transducers glued on the Al resonator base, a quality factor of $Q_{\text{before}} = 1.2 \times 10^6$ at 4.2 K in vacuum with the resonator as machined and $Q_{\text{after}} = 1.05 \times 10^6$ after the deposition of a 600 nm thick Nb film. The reduction of the mechanical quality factor is less than 20%, but Q_{after} still fulfils the requirement, $Q \approx 1.0 \times 10^6$, for the MiniGRAIL transducer. In order to evaluate the effect of a magnetic field on the mechanical quality factor and the electrical quality factor of the Nb circuit, we are planning to test the AL5056 resonator with the Nb persistent coil in the near future.

Figure 6 shows the expected burst strain sensitivity of MiniGRAIL operating at 20 mK equipped with a two-mode inductive transducer with a mechanical quality factor of $Q_{\text{mech}} = 10^6$ and a superconducting pick-up circuit with an electrical quality factor of $Q_{\text{elec}} = 10^5$. In this calculation, the effective

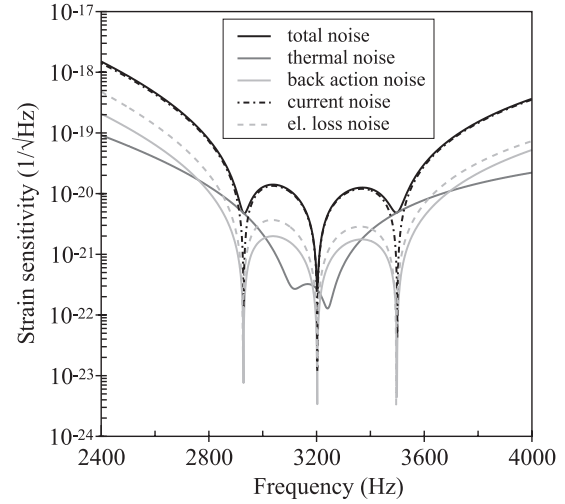


Figure 6. Burst strain sensitivity for MiniGRAIL with a two-mode inductive transducer at $T = 20$ mK and a SQUID amplifier with an energy resolution of $\varepsilon = 3 h$.

pick-up inductance is taken to be $L_{\text{eff}} = 250$ nH, the persistent current is $I_t = 4$ A and the energy resolution of the SQUID is $\varepsilon = 3 h$. Close to the resonances, the sensitivity is limited by the thermal excitation of the mechanical modes. Outside the resonances, the sensitivity is limited by the current noise of the SQUID. The contribution of the back action noise (related to the voltage noise of the SQUID) and the electrical noise (related to the electrical losses in the superconducting circuit) are negligible in a reasonable large bandwidth.

3. Two-stage SQUID systems for MiniGRAIL

The two-stage SQUID systems that are used for the readout of the MiniGRAIL are based on the integrated systems described in [5]. Contrary to the two-stage SQUID systems for the readout of gravitational wave antennae described in [8] and [9], a two-stage SQUID system based on a DROS does not require flux modulation. The sensor SQUID of our system has a SQUID inductance of $L_{\text{sq},1} = 200$ pH, and the DROS has a signal SQUID inductance of $L_{\text{sq},2} = 550$ pH. The white noise of the DROS at $T = 4.2$ K is $\sim 6 \mu\Phi_0 \text{ Hz}^{-1/2}$. The flux gain between the sensor and the DROS is $G_\Phi \approx 36$. The overall white noise level of the two-stage SQUID system at 4.2 K is determined by the sensor SQUID and was measured to be $1.3 \mu\Phi_0 \text{ Hz}^{-1/2}$, corresponding to an energy resolution of $\varepsilon = 27 h$. Based on a flux gain of ~ 36 , the noise contribution of the DROS can be calculated as $(6 \mu\Phi_0 \text{ Hz}^{-1/2})/36 = 0.17 \mu\Phi_0 \text{ Hz}^{-1/2}$, i.e. much smaller than the noise level of the sensor SQUID.

The sensor SQUID and the DROS of the two-stage SQUID systems for the MiniGRAIL consist of two separate chips and are mounted on two separate printed circuit boards (PCBs). This allows a higher design flexibility than the integrated two-stage SQUID systems [5, 6] which integrate the sensor SQUID and the DROS on one single chip. The sensor SQUID is biased at a constant voltage using a thin film RF sputtered Pd resistor with a resistance of $\sim 0.5 \Omega$. In order to damp microwave resonances in the input coils of the sensor SQUID

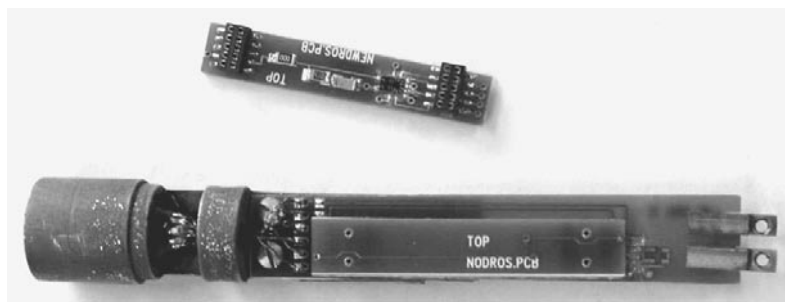


Figure 7. Photograph of the two-stage SQUID modules. The top part shows the printed circuit board on which the DROS is mounted.

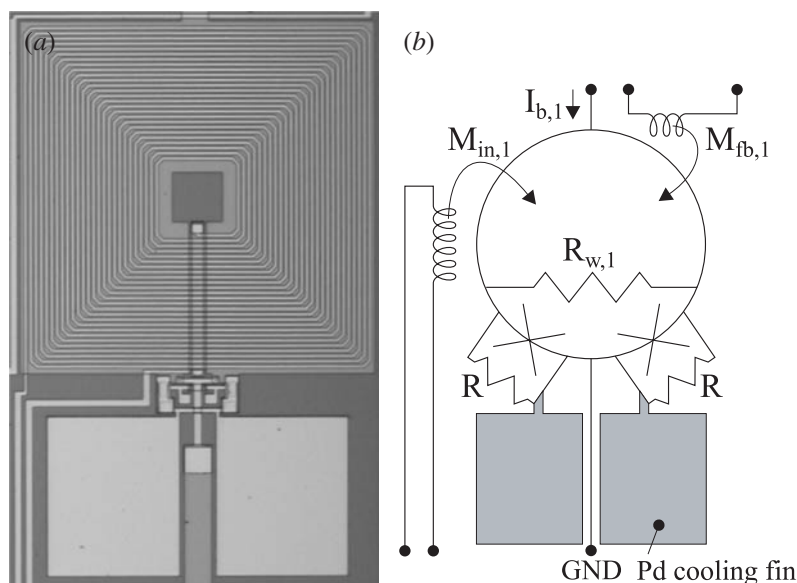


Figure 8. Micrograph (a) and scheme (b) of the sensor SQUIDs with Pd cooling fins (grey blocks) added to the shunt resistors.

and the DROS, external R_{in} - C_{in} shunts of $R_{in} = 50 \Omega$ and $C_{in} = 1 \text{ nF}$ are connected across the input coil. The two-stage SQUID systems are shielded by a cylindrical niobium shield with a length of 90 mm and a diameter of 15 mm to prevent disturbances due to external electromagnetic noise. Figure 7 shows a photograph of the prototype SQUID modules for the MiniGRAIL.

4. Towards nearly quantum limited SQUIDs

In order to improve the energy resolution, the SQUID modules will be operated at the same temperature as the sphere of the gravitational wave detector, i.e. $T \approx 20 \text{ mK}$. Since the energy resolution of a dc SQUID scales linearly with temperature [10], it is expected that at this temperature the energy resolution of the sensor SQUIDs reaches the quantum limit. The first experiments performed on two-stage SQUID systems operating in a dilution refrigerator have been performed, but the SQUIDs have not been operated at 20 mK yet due to insufficient cooling. In order to improve the cooling of the SQUID modules, the design is currently being optimized.

The insufficient cooling of the SQUID modules has several causes. First of all, the wires between the SQUIDs and the room temperature electronics are low pass filtered to

prevent radio frequency interference (RFI) using filters inside the SQUID modules. This caused excessive Joule heating and prevented the SQUIDs to be cooled down to the mK range. In the future, the RFI filters will be placed at a higher temperature, e.g., at the 1 K pot of the dilution refrigerator or at room temperature. Secondly, the hot-electron effect [11] may also limit the sensitivity of the SQUIDs at low temperatures. For this reason, new sensor SQUIDs with Pd cooling fins added to the shunt resistors have been developed. In this way, hot electron may diffuse out and relax in these fins, such that the hot electron effect can be reduced. Since the noise contribution of the DROS is much smaller than the noise of the sensor SQUID, no cooling fins are required for the DROS. Figure 8 shows a micrograph and the corresponding scheme of a sensor SQUID with cooling fins. The SQUID inductance is $L_{sq,1} = 200 \text{ pH}$ and on top of the washer, a 26-turns input coil was deposited. These SQUIDs have been fabricated and will be characterized in a dilution refrigerator in the near future.

5. Conclusion

The MiniGRAIL is the first spherical gravitational wave detector and will be read out by two-stage SQUID systems based on a DROS as the second stage. The two-stage SQUID

systems are coupled to the MiniGRAIL via two coupled mechanical resonators and a persistent current circuit. A prototype Nb flat coil has been developed. The maximum persistent current that could be stored in the coil was 4 A. Prototype two-stage SQUID modules have been developed and characterized at 4.2 K. At this temperature, the overall white energy resolution SQUID system was measured to be $\varepsilon = 27 h$. This corresponds to the theoretical value of the energy resolution of the sensor SQUID [5]. By optimizing the SQUID modules, it is expected that the energy resolution of the two-stage SQUID systems can approach the quantum limit around 20 mK.

References

- [1] De Waard A, Gottardi L and Frossati G 2002 *Class. Quantum Grav.* **19** 1935–41
- [2] De Waard A, Gottardi L, Van Houwelingen J, Shumack A and Frossati G 2003 *Class. Quantum Grav.* **20** S143–51
- [3] Aguiar O D *et al* 2002 *Class. Quantum Grav.* **19** 1949–53
- [4] Gottardi L, De Waard A and Frossati G 2002 *Class. Quantum Grav.* **19** 1943–8
- [5] Podt M, Van Duuren M J, Hamster A W, Flokstra J and Rogalla H 1999 *Appl. Phys. Lett.* **75** 2316–8
- [6] Podt M, Flokstra J and Rogalla H 2002 *Physica C* **372–376** 225–8
- [7] Podt M 2003 *Ph D Dissertation* Faculty of Science and Technology, University of Twente, Enschede, The Netherlands online at <http://www.utwente.nl/webdocs/tn/1/t000001f.pdf>
- [8] Vinante A, Mezzena R, Prodi G A, Vitale S, Cerdonio M, Falferi P and Bonaldi M 2001 *Appl. Phys. Lett.* **79** 2597–9
- [9] Vinante A, Bonaldi M, Falferi P, Cerdonio M, Mezzena R, Prodi G A and Vitale S 2002 *Physica C* **368** 176–80
- [10] Tesche C D and Clarke J 1977 *J. Low Temp. Phys.* **29** 301–31
- [11] Wellstood F C, Urbina C and Clarke J 1989 *Appl. Phys. Lett.* **54** 2599–601